2, 3-Dimercaptosuccinic Acid-Modified Iron Oxide Clusters for Magnetic Resonance Imaging

FEI XIONG,[1] CAIYUN YAN,[1] JILAI TIAN,[1] KUNKUN GENG,[1] ZIYI ZHU,[1] LINA SONG,[1] YU ZHANG,[1] MATTHEW MULVALE,[2] NING GU[1]

[1]State Key Laboratory of Bioelectronics, Jiangsu Laboratory for Biomaterials and Devices, School of Biological Science and Medical Engineering, Southeast University, Nanjing 210096, China

[2]Department of Chemistry, Faculty of Engineering, University of Waterloo, Ontario N2L 3G1, Canada

Received 21 May 2014; revised 17 September 2014; accepted 22 September 2014

Published online 21 October 2014 in Wiley Online Library (wileyonlinelibrary.com). DOI 10.1002/jps.24209

ABSTRACT: Over the last decade, various magnetic nanomaterials have been developed as magnetic resonance imaging (MRI) contrast agents; the greatest challenges encountered for clinical application have been insufficient stability. In this paper, a lyophilization method for 2, 3-dimercaptosuccinic acid-modified iron oxide (γ-Fe_2O_3@DMSA) nanoparticles was developed to simultaneously overcome two disadvantages; these include insufficient stability and low-magnetic response. After lyophilization, the clusters of γ-Fe_2O_3@DMSA with the size of 156.7 ± 15.3 nm were formed, and the stability of the lyophilized powder (γ-Fe_2O_3@DMSA-LP) increased up to over 3 years. It was also found that rehydrated γ-Fe_2O_3@DMSA-LP could be ingested by RAW264.7 cells in very large quantities. Results of pharmacokinetics and biodistribution studies *in vivo* indicated that γ-Fe_2O_3@DMSA-LP is a promising liver-targeted material. Furthermore, it also exhibited higher MRI efficiency and longer imaging time in the liver than the well-known product Feridex®. Moreover, results of vascular irritation and long-term toxicity experiments demonstrated γ-Fe_2O_3@DMSA-LP could be a nontoxic, biocompatible contrast agent *in vivo*. Therefore, the proposed γ-Fe_2O_3@DMSA-LP can be used as a potential MRI contrast agent in clinic for hepatic diseases. © 2014 Wiley Periodicals, Inc. and the American Pharmacists Association J Pharm Sci 103:4030–4037, 2014

Keywords: superparamagnetic iron oxide nanoparticles (SPION); lyophilization; liver targeting; pharmacokinetics; biodistribution; MRI; Formulation; Nanotechnology; Stability

INTRODUCTION

For a long time, drugs were considered as chemical substance used in treatment for diseases; therefore, diagnostic drugs in research of pharmaceutical sciences have been ignored. For safe and effective use of diagnostic drugs in patients, a suitable dosage is required as with most therapeutic drugs. On the contrary, hepatic diseases, including hepatocellular carcinoma, hepatic cyst, and hepatic hemangioma,[1] do not always cause obvious and wide morphologic abnormalities. This means that the diagnosis of qualitative imaging plays an important role in the treatment of liver diseases.

Magnetic resonance imaging (MRI) is an imaging technique used primarily in clinic to produce high-quality images of the inside of human body based on the different relaxation times of hydrogen atoms.[2] Currently, the most used contrast agent for MRI in clinic is a gadolinium (Gd) chelate, for example, Magnevist® (gadopentetate dimeglumine), but the *in vivo* distribution is not specific, and the elimination occurs too quickly, and what is worse is that parts of patients appeared adverse reaction of nephrogenic systemic fibrosis. Therefore, high-sensitivity MRI contrast agent is in urgent need to provide additional contrast for liver from other tissues.

Currently, there are only two liver-targeting MRI contrast agents used in clinic, dextran or carboxydextran-coated magnetite colloidal particles (Feridex® and Resovist®). On the nanoscale, magnetic particles possess a strong tendency to agglomeration because of its high-specific surface area and interaction induced by magnetism. Increasing particle size and/or increasing saturation magnetization directly increases aggregation and sedimentation of magnetic nanoparticles dispersion. This aggregation is amplified during the long-term storage in aqueous solution. The physical and chemical instability is the greatest challenge of nanoparticule systems involving liposomes, solid nanoparticles, and nanoemulsion, which will lead to precipitation and degradation. Surface modification and reduction in the size distribution are typical methods for obtaining stable nanoparticule systems. Both aforementioned contrast agents can be stabilized by using macromolecular coatings (polymers, such as dextran and carboxydextran) and by maintaining a monodisperse size to resist aggregation. However, this kind of nanoparticular colloid is generally complex, cost-consuming, and requires several separation steps to obtain pure macromolecules, resulting in very low yield.

Lyophilization, also known as freeze-drying, is a wise industrial process, which removes water from a frozen sample by sublimation and desorption under vacuum. Compared with other drying methods, lyophilization has the advantage of not damaging to temperature- or oxidative-sensitive materials and can limit bacterial growth. Above all, once the free water was removed completely, nanoparticles can be stored for long periods of time and can be transported conveniently. There are lots of lyophilized liposomal drugs used in the clinic, such as AmBisome® (NeXstar Pharmaceuticals Inc., Boulder, USA) and Myocet™ (Elan Pharmaceuticals Inc., Princeton, NJ, USA).[3] In this paper, we selected small molecular

Correspondence to: Ning Gu (Telephone: +8625-83272476; Fax: +8625-83272460; E-mail: guning@seu.edu.cn)

Journal of Pharmaceutical Sciences, Vol. 103, 4030–4037 (2014)

2, 3-dimercaptosuccinic acid-modified maghemite nanoparticles (γ-Fe_2O_3@DMSA) as liver-targeted contrast agent, which was not easily oxidized as compared with magnetite and can be produced in large quantities by coprecipitation. Lyophilization technology of γ-Fe_2O_3@DMSA developed here could simultaneously produce clusters of γ-Fe_2O_3@DMSA and turn the colloid into powder. It is reported that the iron oxide clusters showed higher magnetic response and a considerable increase in MRI relaxivity than that of individual ones because of the interaction between the aggregated nanocrystals.[4–7] Therefore, the lyophilized powder (γ-Fe_2O_3@DMSA-LP) was expected not only to improve the stability, but also enhance the MRI contrast efficiency.

In this study, the cellular uptake *in vitro*, pharmacokinetics, and biodistribution *in vivo* were sequentially investigated to explore the mechanism of liver targeting. The MRI and toxicity experiments were conducted and revealed that the proposed γ-Fe_2O_3@DMSA-LP could be used as a potential biocompatible MRI contrast agent in clinic for hepatic diseases.

MATERIALS AND METHODS

Materials

All the chemicals were purchased from Sinopharm Chemical Reagent Company, Ltd. (SCRC, Shanghai, China) unless otherwise specified. $(CH_3)_4NOH$ and DMSA were purchased from Shanghai Zhuorui Chemical Reagent Company, Ltd. Maltose was purchased from Shanghai Huixing Biochemical Reagent Company, Ltd. Sucrose, polyethylene glycol (PEG 400), dextran, glycine, and leucine were purchased from Sinopharm Chemical Reagent Company, Ltd. Poly vinyl pyrrolidone (PVP K30) was purchased from BASF (BASF Corporation, Mount Olive, N.Y.). RAW264.7 cells were purchased from Shanghai Cellular Institute of China Scientific Academy. RPMI 1640 medium (containing 10% fetal calf serum, 100 μg mL^{-1} penicillin, and 100 μg mL^{-1} streptomycin), glucose-free RPMI 1640 medium, and fetal calf serum were purchased from Shanghai BoooCle Biopharm Company, Ltd. All the chemicals were of analytical reagent grade.

Male white rabbits (1.6–2.2 kg) and male SD mice (18–22 g) were obtained from Animal Experiment Center of Southeast University. Animal experiments were performed via a protocol approved by the Institutional Animal Care and Use Committee of Southeast University.

Methods

Preparation of γ-Fe_2O_3@DMSA-LP

γ-Fe_2O_3 were synthesized by chemical coprecipitation and subsequently coated with DMSA as previously described.[8] Briefly, a mixed solution of $FeCl_3 \cdot 6H_2O$ (0.01 M) and $FeSO_4 \cdot 7H_2O$ (0.006 M) was adjusted to pH 9.0 by aqueous ammonia solution (1.5 M) under a N_2 environment. After washing with water and ethanol, the obtained magnetite nanoparticles were dispersed in water and the pH was adjusted to 3.0 using 0.1 M HCl. Then, these magnetite nanoparticles were oxidized into reddish-brown γ-Fe_2O_3 nanoparticles at about 95°C–100°C for 1 h. For DMSA coating, 0.01 M DMSA was added to the γ-Fe_2O_3 nanoparticles solution. Finally, the products were washed repeatedly with water.[9,10]

The preparation of γ-Fe_2O_3@DMSA-LP was performed with a vacuum freeze dryer (FreeZone.6L, Labconco Corp., Kansas City, MO). The γ-Fe_2O_3@DMSA colloidal suspension was mixed with different skeleton materials and stabilizers, followed by being sterilized and prefrozen for 12 h, and finally dried under reduced pressure to remove moisture.

Characterization

Scanning electron microscopy (SEM) was utilized to identify the microstructure of γ-Fe_2O_3@DMSA-LP with a S4800 microscope (Hitachi High Technologies Japan Inc., Tokyo, Japan). X-ray diffraction (XRD) was used to determine the crystal structure of the sample on a *D*/max-rA diffractometer with CuKα radiation (Rigaku Corporation, Tokyo, Japan). The morphology of rehydrated γ-Fe_2O_3@DMSA-LP was observed by transmission electron microscopy (TEM) using a JEM-2100 (JEOL, Tokyo, Japan). Magnetization measurements were carried out with a 7407 vibrating sample magnetometer (Lake Shore, Westerville, OH, USA). The size and zeta potential of the rehydrated γ-Fe_2O_3@DMSA-LP were determined at 25°C by photon correlation spectroscopy instrument (Malvern Zetasizer 3000; Malvern Instruments Company, Worcestershire, UK).

Stability

At 0.5, 1, 2, and 3 years after preparation, γ-Fe_2O_3@DMSA-LP was rehydrated with sterile water. To determine the stability in clinical use, the size, zeta potential, and iron concentration at 0, 4, and 12 h after rehydration were measured.

Intracellular Uptake of Iron

RAW 264.7 cells were seeded in 48-well plates at density of 1.5×10^4 cells per well and left overnight. After exposure to the rehydrated γ-Fe_2O_3@DMSA-LP at concentrations of 50, 100, 200 μg Fe per milliliter in medium at 37°C for 1 h, the cells were washed, stained with 2% potassium ferrocyanide (Perl's reagent), and nuclear fast red. Stained cells were observed with a light microscope (Axioplan Imaging II; Zeiss, Oberkochen, Germany) and photographed.

Pharmacokinetics and Biodistribution

Mice ($n = 3$) were injected via the tail vein with the rehydrated γ-Fe_2O_3@DMSA-LP at a dose of 1.5 mg Fe per kilogram. At several time intervals after injection blood, liver, kidneys, and spleen were collected and digested with HNO_3 and iron concentrations were determined by the *O*-phenanthroline colorimetric method.[10] The determination of iron concentration before injection was for elimination of endogenous iron.

MRI *In Vivo*

Male SD mice ($n = 4$) were injected intravenously through the tail vein with the rehydrated γ-Fe_2O_3@DMSA-LP (5.05 mg Fe kilogram). All mice were examined by MRI at several time intervals after injection. MRI images were measured on an Avanto-1.5T Magnetic Resonance Imaging Equipment (Siemens Healthcare, Erlangen, Germany). Experimental parameters for the spin-echo images were TR 5500 ms, TE 101 ms, 2 NEX, and FOV 14 × 14 cm^2.

Safety Assay

Vascular irritation test were performed as previously described.[11] Rehydrated γ-Fe_2O_3@DMSA-LP (1.85 mg Fe per

kilogram) and normal saline as a control were injected intravenously into the ear-edge of the right and left ears of rabbits ($n = 3$) once a day for 3 days. The injection position was observed 48, 72, 96 h after last administration. Then, rabbits were sacrificed and ears were collected and formalin fixed. The cut was placed near the heart terminal at 1.3, 2.6, and 4.0 cm from the injection position. Then, the ears were paraffin embedded and Hematoxylin-Eosin (HE) stained for evaluation of vascular irritation.

Long-term toxicity tests were performed as previously described.[11] Male SD rats were randomly assigned into four groups ($n = 3$). Rehydrated γ-Fe_2O_3@DMSA-LP (3.5, 5.0, and 6.5 mg Fe per kilogram) and normal saline as a control were injected via the tail-vein once a day for 2 weeks. The weight changes of each rat during administration were recorded. After the last administration, livers and kidneys were collected and HE stained for evaluation of the long-term toxicity.

RESULTS AND DISCUSSION

Preparation of γ-Fe_2O_3@DMSA-LP

In this paper, we used a lyophilized γ-Fe_2O_3@DMSA to overcome insufficient stability and low magnetic response of iron oxide nanoparticles. The increased stability can save many cost-consuming steps of preparation and thus the production cost could be reduced. The formed cluster in the lyophilization process has a higher magnetic response and thus a more efficient imaging of liver can be achieved. The strategy of developing a stable γ-Fe_2O_3@DMSA clusters powder during a lyophilization procedure was shown schematically in Figure 1. In this research, we investigated several skeleton materials, including 5% of glucose, 5% of mannitol (5%), 10% of lactose, 10% of trehalose, 10% of maltose, and 10% of sucrose(w/v). SEM images of lyophilized powder of γ-Fe_2O_3@DMSA are shown in Figure 2. Mannitol proved to build an elegant coherent cake structure with good mechanical properties (Fig. 2a) and the reconstitution process occurred rapidly (5.7 s to reconstitution). Sediment was still observed after rehydration of powder lyophilized with sucrose (Fig. 2b; 9.6 s to reconstitution) or lactose as the skeleton material (Fig. 2c; 8.7 s to reconstitution). Trehalose (Fig. 2d) and maltose (Fig. 2e) took 17.9 and 7.9 s, respectively, to be

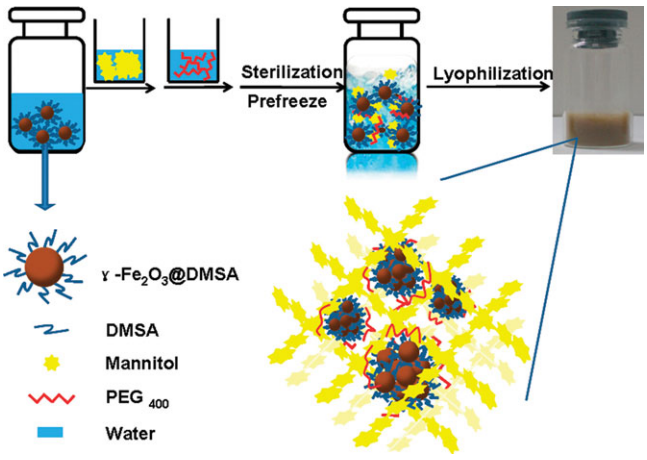

Figure 1. Schematic representation of preparation and structure of γ-Fe_2O_3@DMSA-LP.

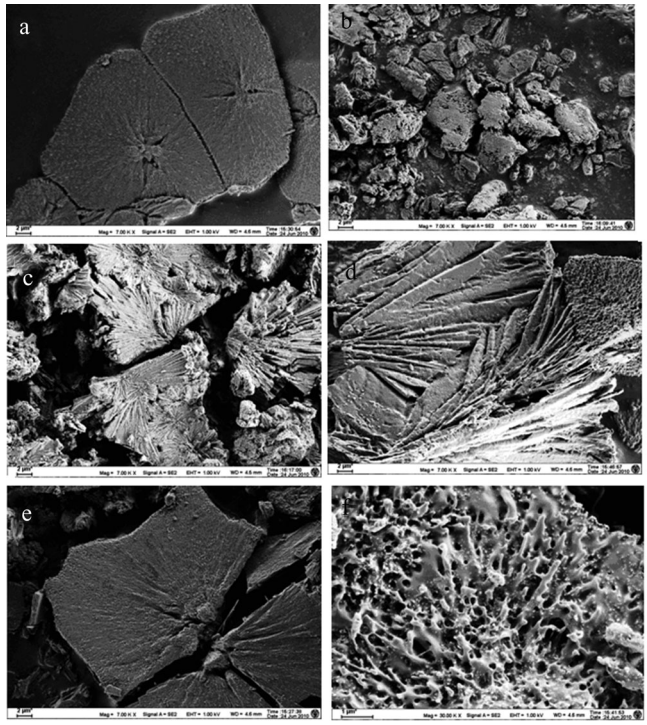

Figure 2. Scanning electronic microscopy images of lyophilized powder of γ-Fe_2O_3@DMSA with different skeleton materials and stabilizer. (a) Mannitol. (b) Sucrose. (c) Lactose. (d) Trehalose. (e) Maltose. (f) PEG 400.

completely dispersed in water and the particle size had dramatically increased after reconstitution (from 46.4 ± 12.3 to 208.6 ± 17.9 nm for powder lyophilized with trehalose and from 48.2 ± 11.8 to 231.1 ± 18.7 nm for powder lyophilized with maltose). The microstructure of powder lyophilized with glucose showed a significant shrinkage and collapse phenomena, and it could not be reconstituted in water (data not shown). Lyophilization is often used to stabilize various pharmaceutical products, including virus vaccines, protein and peptide formulations, and liposome and small chemical drug formulations.[12–15] The study of using the lyophilization method to improve the stability and magnetism effect of magnetic nanoparticles has seldom been reported. The high concentration of particulate in the system may induce aggregation and the crystallization of ice may add mechanical stress on nanoparticles leading to their destabilization. For these reasons, special agents must be added to the colloidal solution of nanoparticles before lyophilization to protect these fragile systems. After getting mixed with skeleton materials and stabilizers, the well-dispersed γ-Fe_2O_3@DMSA colloid aggregated gently into clusters and these clusters were protected separately by skeleton materials from shrinking or collapsing in the freeze-drying process. In addition, high hydrophilic skeleton materials also improved the reconstitution.

Lyophilization process is composed of three steps: freezing (solidification), primary drying (ice sublimation), and secondary drying (desorption of unfrozen water). The drying process, including the physical state changes and movement of the water, occurs in the low temperature and pressure. It is important to protect the nanoparticles during lyophilization against freezing and drying stresses. Several stabilizers, such as polymers, copolymers, and amino acids were screened, including PEG 400,

 DOI 10.1002/jps.24209

PVP K30, dextran, glycine, and leucine (0.5%, w/v). PEG 400 resulted in a porous cake structure (Fig. 2f); thus, the reconstitution speed of lyophilized powder with PEG 400 was fast and the particle size increased gently after lyophilization. After ultrasonication for a long period of time, it was difficult to reconstitute the powder with PVP K30 or dextran. Other stabilizers increased the particle size dramatically (from 50.3 ± 11.8 to 897.5 ± 19.3 nm for powder lyophilized with glycine and from 47.9 ± 15.2 to 924.5 ± 17.7 nm for powder lyophilized with leucine) and caused extreme aggregation. These stabilizers can vitrify at a specific temperature denoted T_g'.[16] The immobilization of nanoparticles within a glassy matrix prevents a aggregation and mechanical stress from the formation of ice crystals. Generally, freezing must be conducted below the T_g' of a frozen amorphous sample, in order to ensure the total solidification of the sample.[17] The T_g' of glucose is the lowest, which makes the reunion between the clusters and the reconstruction difficult. When using lactose or sucrose, the mechanical force generated from crystallization of protective agent made a small amount of agglomerates and the agglomerates could not be redispersed after ultrasonication. The T_g' of mannitol is the highest and its glassy state was seen as a physical barrier in the formation of ice crystals and aggregation of the particles during freeze-drying. Therefore, the immobilizing within the glassy matrix of mannitol is the best way to stabilize the nanoparticles.

After moist heat sterilization under 100°C for 30 min, the particle size of colloidal suspension of γ-Fe_2O_3@DMSA increased to 468.4 ± 21.3 nm and large aggregations could be observed (Fig. 3a). After moist heat sterilization under 121°C for 15 min, the colloidal suspension partly separated into sedimentation layer and water. The suspension could be dispersed again by shaking, but the particles size was up to 835.2 ± 25.3 nm. After lyophilization, particles stuck to each other in the skeleton materials (Fig. 3b) and a lot of sedimentation could be observed in the rehydrated sample. Microvascular thrombosis may occur via intravenous administration. Filter sterilization using 0.22 μm membrane did not lead to significant change in particle size, zeta potential, and stability of γ-Fe_2O_3@DMSA. The lyophilized powder of filtered nanoparticles was multiporous (Fig. 3c) and could be rehydrated easily. Sterilization is one of the essential processes to insure the security of sterile preparation for intravenous administration in clinic; however, there are few reports regarding the sterilization of inorganic nanoparticles. The sterilization results in this paper indicated that 0.22 μm membrane filtration was the best sterilization method for magnetic nanoparticle materials for further clinical application.

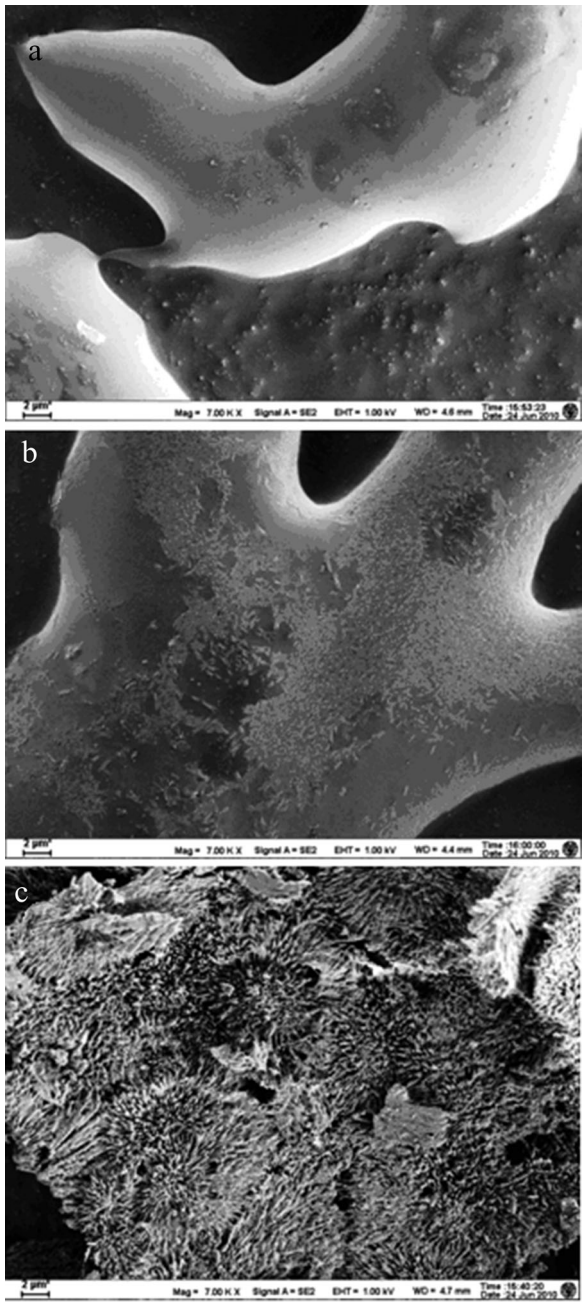

Figure 3. Scanning electron microscopy images of γ-Fe_2O_3@DMSA-LP after sterilization by different methods. (a) Moist heat sterilization under 100°C for 30 min. (b) Moist heat sterilization under 121°C for 15 min. (c) 0.22 μm membrane filter sterilization.

Characterization of γ-Fe_2O_3@DMSA-LP

Fourier transform infrared (FT-IR) spectra of DMSA, γ- Fe_2O_3, and γ- Fe_2O_3@DMSA nanoparticles are shown in Figure 4a. The band at 3370 cm^{-1} in the FT-IR curve of γ-Fe_2O_3@DMSA corresponded to S–H stretching vibration. The band at 1390 and 1610 cm^{-1} corresponded to COO symmetric and asymmetric stretching vibration, respectively, which indicated the carboxy group coordinating to the metal in monodentate mode. The Fe–O stretching vibration appeared in the region 561 and 631 cm^{-1}. FT-IR results confirm the successful surface DMSA modification of γ-Fe_2O_3 nanoparticles. XRD pattern of γ-Fe_2O_3@DMSA nanoparticles shown in Figure 4b displays six broad peaks appearing at 2θ 31°, 36°, 43°, 54°, 58°, and 62°. All the observed diffraction peaks could be indexed by the cubic structure of Fe_2O_3 (JCPDS No.39-1346). The hysteresis loop with zero coercivity and remanence shown in Figure 4c indicated superparamagnetic behavior of γ-Fe_2O_3@DMSA nanoparticles after lyophilization. The saturation magnetization value (Ms) of γ-Fe_2O_3@DMSA nanoparticles after lyophilization was 65.35 emu g^{-1}. TEM in Figures 4d and 4e showed the γ-Fe_2O_3@DMSA nanoparticles before lyophilization and the clusters of rehydrated γ-Fe_2O_3@DMSA-LP, respectively. To prepare a TEM sample for imaging, the nanoparticles colloid was

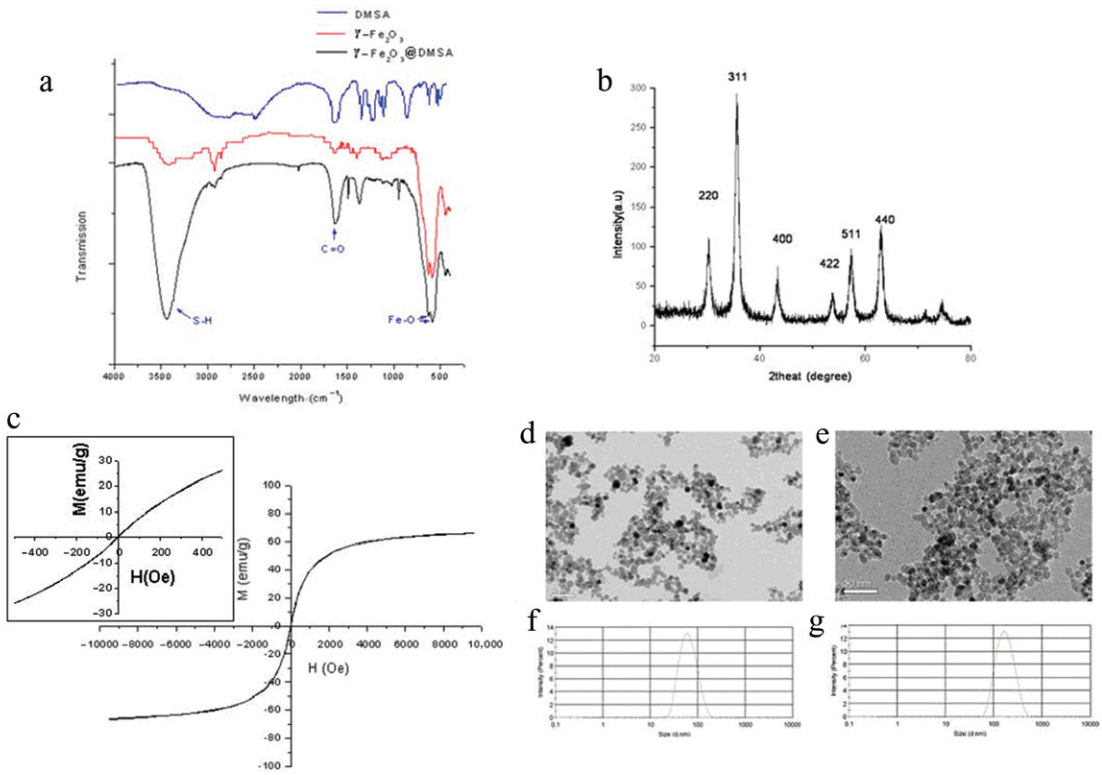

Figure 4. Characterization of γ-Fe_2O_3@DMSA-LP. (a) FT-IR spectra of DMSA, γ-Fe_2O_3, and γ-Fe_2O_3@DMSA nanoparticles. (b) XRD pattern of γ-Fe_2O_3@DMSA nanoparticles. (c) The hysteresis loop of γ-Fe_2O_3@DMSA-LP. (d) TEM image of γ-Fe_2O_3@DMSA. (e) TEM image of rehydrated γ-Fe_2O_3@DMSA-LP. (f) Hydrodynamic diameter distribution of γ-Fe_2O_3@DMSA. (g) Rehydrated γ-Fe_2O_3@DMSA-LP.

dried onto a carbon-coated copper grid and capillary drying forces brought the particles into aggregates, which made it appear to be agglomerated and therefore the size is larger than hydrodynamic diameter. The average hydrodynamic diameter of γ-Fe_2O_3@DMSA and rehydrated γ-Fe_2O_3@DMSA-LP was 45.3 ± 11.2 and 156.7 ± 15.3 nm (Figs. 4f and 4g), respectively. The PDI value of γ-Fe_2O_3@DMSA and rehydrated γ-Fe_2O_3@DMSA-LP was 0.127 and 0.168, respectively. The zeta potential of rehydrated γ-Fe_2O_3@DMSA-LP was −(32.2 ± 2.0) mV, which could provide enough electrostatic repulsion around particles when they were in a water medium to ensure there was no sediment or block in the syringes during clinical injection.

As lyophilized powder is required to be rehydrated with a solution to a particle-free clarified solution for parenteral administration such as intravenous, intramuscular, intraperitoneal, or subcutaneous injection, it is important to investigate the stability of γ-Fe_2O_3@DMSA-LP after reconstruction. After 0.5, 1, 2, and 3 years storage of γ-Fe_2O_3@DMSA-LP at room temperature (range from 0°C to 38°C in four seasons over 3 years), the Fe content, particle size, zeta potential, and Ms of γ-Fe_2O_3@DMSA-LP after reconstitution did not change significantly, and the average percentage RSD (relative standard deviation) of measured parameters was within 8%. The particle size ranged from 152.1 ± 13.7 to 166.3 ± 18.2 nm and zeta potential ranged from −(30.5 ± 2.3) to −(32.8 ± 2.1) mV within 24 h after rehydration. All the above results indicated this contrast agent with good stability is easily stored and used, which is important for further clinical applications of MRI.

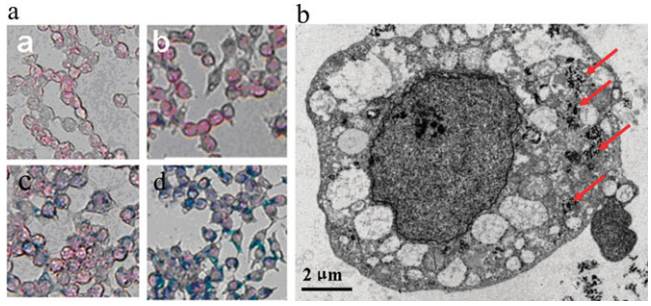

Figure 5. *In vitro* cellular uptake of rehydrated γ-Fe_2O_3@DMSA-LP in RAW 264.7 cells. (a) Prussian blue and nuclear fast red double staining images of cells at concentrations of 0 μg mL^{-1} (a), 50 μg mL^{-1} (b), 100 μg mL^{-1} (c), and 200 μg mL^{-1} (d) of rehydrated γ-Fe_2O_3@DMSA-LP in medium at 37°C for 1 h (magnification 400×). (b) TEM of cells incubated with 100 μg mL^{-1} of rehydrated γ-Fe_2O_3@DMSA-LP in medium at 37°C for 1 h.

Cellular Uptake by Macrophage Cells

To assess macrophage uptake, such as reticuloendothelial system (RES) and mononuclear phagocyte system (MPS), *in vitro* phagocytosis experiments were carried out using RAW 264.7 macrophage cells prior to *in vivo* studies. Figure 5a showed the optical micrographs of prussian blue-stained RAW264.7 cells. Most of the RAW 264.7 cells incubated with 50, 100, and 200 μg mL^{-1} of rehydrated γ-Fe_2O_3@DMSA-LP for 1 h exhibited blue staining, and the uptake was concentration dependent. TEM

 DOI 10.1002/jps.24209

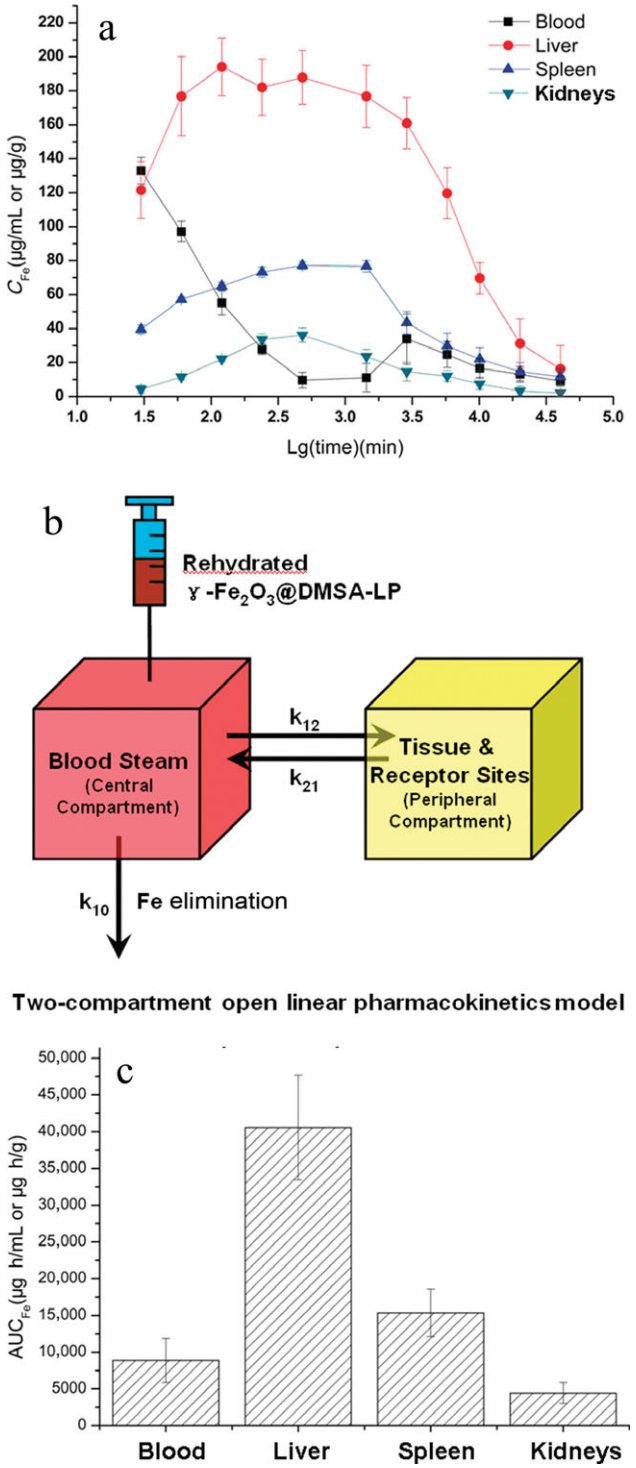

Figure 6. *In vivo* pharmacokinetics and tissue distribution of γ-Fe_2O_3@DMSA-LP in mice. (a) Curves of Fe concentration versus time in blood, liver, spleen, and kidneys of mice receiving an intravenous injection of 1.5 mg kg^{-1} of rehydrated γ-Fe_2O_3@DMSA-LP (n = 3). (b) Scheme of two-compartment open linear pharmacokinetic mode: k21, the first-order rate constant from peripheral compartment to central compartment; k10, the first-order elimination rate constant from central compartment; k12, the first-order rate constant from central compartment to peripheral compartment; (c) AUC of Fe in blood, liver, spleen, and kidneys of mice.

Table 1. The Pharmacokinetics Parameters of Fe in Mice Blood After Intravenous Administration of Rehydrated γ-Fe_2O_3@DMSA-LP

Parameters	Value	Parameters	Value
$t_{1/2(\alpha)}$ (h)	1.051	V_c (mL)	84.257
$t_{1/2(\beta)}$ (h)	34,693.836	Cl_s (mL h^{-1})	0.026
k_{21} (1/h)	0.042	$AUC_{0\to\infty}$ (μg h mL^{-1})	16,530.100
k_{10} (1/h)	0.311×10^{-3}	$MRT_{0\to\infty}$ (h)	858.739
k_{12} (1/h)	0.617		

$t_{1/2(\alpha)}$, distribution half-life; $t_{1/2(\beta)}$, elimination half-life; k_{21}, the first-order rate constant from peripheral compartment to central compartment; k_{10}, the first-order elimination rate constant from central compartment; k_{12}, the first-order rate constant from central compartment to peripheral compartment; V_c, apparent volume of distribution; Cls, systemic clearance; $AUC_{0\to\infty}$, area under the curve from 0 h to infinity; $MRT_{0\to\infty}$, mean residence time from 0 h to infinity.

image of cells (Fig. 5b) shows that the majority of rehydrated γ-Fe_2O_3@DMSA-LP are located in lysosomes, which is consistent with previous studies.[18,19]

Pharmacokinetics and Biodistribution

The concentration–time curve of Fe in plasma of mice with intravenous administration of rehydrated γ-Fe_2O_3@DMSA-LP is shown in Figure 6a. 3P97 pharmacokinetic program was used to analyze the curve, and the plasma data were characterized with a two-compartment model with linear elimination (Fig. 6b). The main pharmacokinetics parameters are listed in Table 1. Results show γ-Fe_2O_3@DMSA has a short distribution half-life ($t_{1/2(\alpha)}$ = 1.051 h), long elimination half-life ($t_{1/2(\beta)}$ = 34,693.836 h) and slow elimination rate (Cl_s = 0.026 mL h^{-1}) from blood. The first-order rate constant from the central compartment to the peripheral compartment (k_{12}) was 14.69 times faster than that from the peripheral compartment to the central compartment (k_{21}), which indicated that the γ-Fe_2O_3@DMSA preferred to be distributed to the peripheral compartment (all tissue spaces outside the central compartment) from the central compartment (blood). The area under the curve (AUC) corresponds to the integral of the blood concentration versus an interval of time. Mean residence time (MRT) is an important parameter, which represented the time required for 63.2% of the dose to be eliminated from the body. The AUC and MRT were calculated using noncompartmental analysis, indicated that γ-Fe_2O_3@DMSA could stay in body over 1 month with enough dose for MRI, and the patients did not need to examine the MRI immediately after injection.

The RES organs, such as the liver, play the major responsibility in clearing small exogenous particles from blood, which is often employed in passive targeting. The AUC of γ-Fe_2O_3@DMSA distributed in different tissues is shown in Figure 6c. The AUC value of liver is 4.576 and 9.120 times larger than that of blood and kidneys, respectively. In the liver, iron oxide nanoparticles were taken up by macrophages, and were only found in healthy liver tissues but not in pathological tissues, such as primary liver cancer, metastases, cysts, adenomas, and hyperplasia. Consequently, there are significant differences in relaxation between normal tissue (decreased signal intensity) and lesions (native signal intensity), resulting in increased sensitivity for detection of focal liver lesions. Results of cellular uptake by macrophage cells *in vitro* indicated that rehydrated γ-Fe_2O_3@DMSA-LP could be rapidly opsonized and uptaken

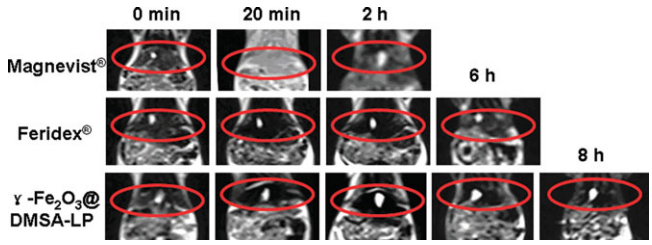

Figure 7. Magnetic resonance images of mice at different times after receiving an intravenous injection of different contrast agents. (a) 0.9 mmol kg^{-1} of Magnevist® (T1 weighted). (b) 5.05 mg kg^{-1} of Feridex® (T2 weighted). (c) 5.05 mg kg^{-1} of rehydrated γ- Fe_2O_3@DMSA-LP (T2 weighted).

by RES- and MPS-rich organs after intravenous administration. After being injected into the venous system *in vivo*, γ-Fe_2O_3@DMSA is largely phagocytized by hepatic and splenic macrophages and thus γ-Fe_2O_3@DMSA was distributed mainly in the liver and spleen. Results of AUC in different tissues indicated that γ-Fe_2O_3@DMSA-LP possessed higher accumulation in liver and was a candidate for MRI of liver diseases.

MRI *In Vivo*

The MRI of mice injected via tail vein with Magnevist® (0.9 mmol kg^{-1}) and Feridex® (the same dose of Fe) were examined as control. T1- and T2-weighted MRI of mice *in vivo* are presented in Figure 7. Liver signal intensity among three groups was almost same before injection (0 min) and the liver contour could be seen clearly. At 20 min after injection of Magnevist®, the imaging of the majority of the tissue appeared bright, which indicated it was a nontargeted contrast agent in T1-weighted imaging and could not provide information on the extent of the liver damage. At 2 h after injection, the signal intensity on T1-weighted MRI images was recovered. For Feridex® group, the signal intensity of liver (T2-weighted imaging) was greatly reduced at 20 min and 2 h after administration. At 6 h after injection, the signal intensity of liver had almost recovered and contrast-enhanced images could not be observed anymore. For γ-Fe_2O_3@DMSA-LP group, the signal intensity (T2-weighted imaging) was also greatly reduced at 20 min, 2, and 6 h, and liver image of 2 h group was darker than that of Feridex® group at the same time. Although the signal intensity recovered continually from 6 to 8 h after injection, the contrast effect was also evident at 8 h. The signal returned to normal gradually after 8 h.

To assess the application potentials of γ-Fe_2O_3@DMSA-LP in liver imaging and accumulation ability in liver *in vivo*, the MRI of mice treated with rehydrated γ-Fe_2O_3@DMSA-LP solution was carried out at different intervals after injection. MRI results indicated that γ-Fe_2O_3@DMSA-LP can potentially enhance the efficacy of early diagnosis and its contrast-enhanced imaging of liver can last for a longer time than that of Feridex®.

Safety Evaluation

Results of gross observations showed in Figure 8a that there were no swelling, bleeding, edemas, and inflammation on the injection site from 48 to 96 h. There were also no swelling, thrombus, vascular congestion, and inflammatory cell infiltration observed at 1.3, 2.6, and 4.0 cm from injection site after

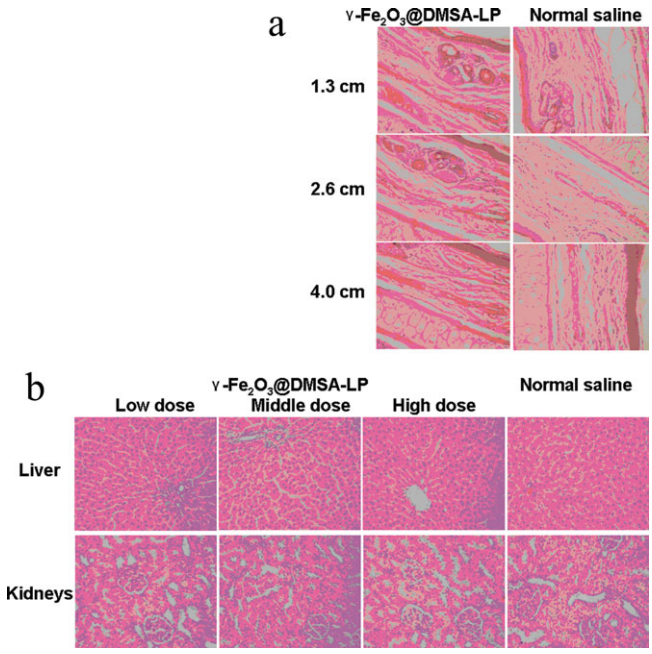

Figure 8. Systemic toxicity of γ-Fe_2O_3@DMSA-LP in mice (magnification 400×). (a) Representative pathology slide photomicrographs of rabbit ear vein slices in vascular irritation test. (b) Representative histological HE staining photomicrographs of liver and kidney slices of mice after intravenous injection for 14 days (once a day).

injection with rehydrated γ-Fe_2O_3@DMSA-LP at the dosage of 1.85 mg Fe per kilogram.

Microphotographs of the HE-stained liver and kidneys sections of rat after once-daily injection for 2 weeks are shown in Figure 8b. Liver cells of normal saline group were arranged in cords. Liver slices of three doses groups of γ-Fe_2O_3@DMSA-LP showed the liver cells were also arranged in cords and no necrosis or degeneration was observed. The results of kidneys slice showed no significant difference among normal saline group and different doses groups of γ-Fe_2O_3@DMSA-LP. There was also no serious body weight loss of mice treated with γ-Fe_2O_3@DMSA-LP (data not shown).

A significant hazard of intravenous injection is vascular irritation, a kind of side effect that can impose relevant delays in preclinical and clinical use. Vascular irritation assays are very important for injection before performing animal experiments and clinical trial because vessels and erythrocytes are initially parts of the body meeting and interacting with intravenous injection. The vascular irritation of iron oxide nanoparticles has not been reported till date. For one-time and single dose-administrated contrast agent, toxicity tests for 2 weeks can be used as long-term toxicity assay. Results of long-term toxicity as well as vascular irritation demonstrated that the toxicity of γ-Fe_2O_3@DMSA-LP in rat was not significant and γ-Fe_2O_3@DMSA-LP could be a safe MRI contrast agent.

CONCLUSIONS

In this research, we used lyophilization method developed here to simultaneously produce clusters of γ-Fe_2O_3@DMSA and change the colloid into a powder. This method is simple to perform, feasible for clinical applications, has low costs, and keeps

 DOI 10.1002/jps.24209

nanoparticles stable for more than 3 years. *In vitro* and *in vivo* studies showed γ-Fe_2O_3@DMSA-LP could be uptaken in high concentrations by macrophage cells and by the liver. The MR contrast-enhanced imaging can potentially enhance the efficacy of early diagnosis, and the image contrast of the liver is more effective than current products used in clinics today. Toxicity assay also showed it was safe and compatible. The proposed γ-Fe_2O_3@DMSA-LP with small molecular coatings, low cost, massive production process without special separation, and perfect stability makes it convenient for use in clinic, and can pave the way to be potentially used as an MRI contrast agent in clinics for hepatic diseases.

ACKNOWLEDGMENTS

This work was financially supported by National Basic Research Program of China (No. 2011CB933503 and 2013CB934400), National Natural Science Foundation of China (No. 81473160, 81172955, and 81302773), the Fundamental Research Funds for the Central Universities (2242014R30013 and 22420135002), School of Pharmacy, Fudan University, and The Open Project Program of Key Lab of Smart Drug Delivery (Fudan University), Ministry of Education, China.

REFERENCES

1. Darvesh AS, Aggarwal BB, Bishayee A. 2012. Curcumin and liver cancer: A review. Curr Pharm Biotechnol 13(1):218–228.
2. Haacke EM, Brown RW, Thompson MR, Venkatesan R. 1999. Magnetic resonance imaging: Physical principles and sequence design. New York: John Wiley and Sons.
3. Arshinova OY, Sanarova EV, Lantsova AV, Oborotova NA. 2012. Lyophilization of liposomal drug forms (review). Pharm Chem J 46(4):228–233.
4. Ge J, Hu Y, Biasini M, Beyermann WP, Yin Y. 2007. Superparamagnetic magnetite colloidal nanocrystal clusters. Angew Chem Int Ed 46(23):4342–4345.
5. Kim J, Lee JE, Lee SH, Yu JH, Lee JH, Park TG, Hyeon T. 2008. Designed fabrication of a multifunctional polymer nanomedical platform for simultaneous cancer-targeted imaging and magnetically guided drug delivery. Adv Mater 20(3):478–483.
6. Niu D, Li Y, Ma Z, Diao H, Gu J, Chen H, Zhao W, Ruan M, Zhang Y, Shi J. 2010. Preparation of uniform, water-soluble, and multifunctional nanocomposites with tunable sizes. Adv Funct Mater 20(5):773–780.
7. Qiu P, Jensen C, Charity N, Towner R, Mao C. 2010. Oil phase evaporation-induced self-assembly of hydrophobic nanoparticles into spherical clusters with controlled surface chemistry in an oil-in-water dispersion and comparison of behaviors of individual and clustered iron oxide nanoparticles. J Am Chem Soc 132(50):17724–17732.
8. Molday RS. 1984. Magnetic iron-dextran microspheres. Patent US4452773A.
9. Fauconnier N, Pons JN, Roger J, Bee A. 1997. Thiolation of maghemite nanoparticles by dimercaptosuccinic acid. J Colloid Interface Sci 194(2):427–433.
10. Xiong F, Zhu Z, Xiong C, Hua X, Shan X, Zhang Y, Gu N. 2012. Preparation, characterization of 2-deoxy-D-glucose functionalized dimercaptosuccinic acid-coated maghemite nanoparticles for targeting tumor cells. Pharm Res 29(4):1087–1097.
11. Xiong F, Xiong C, Yao J, Chen X, Gu N. 2011. Preparation, characterization and evaluation of breviscapine lipid emulsions coated with monooleate–PEG–COOH. Int J Pharm 421(2):275–282.
12. Mozhaev VV, Martinek K. 1984. Structure–stability relationships in proteins: New approaches to stabilizing enzymes. Enzyme Microb Tech 6(2):50–59.
13. Pikal MJ. 1990. Freeze-drying of proteins. Part II: Formulation selection. Bio Pharm 3(9):26–30.
14. Colaco C, Sen S, Thangavelu M, Pinder S, Roser B. 1992. Extraordinary stability of enzymes dried in trehalose: Simplified molecular biology. Biotechnology 10(9):1007–1011.
15. Cleland JL, Lam X, Kendrick B, Yang J, Yang TH, Overcashier D, Brooks D, Hsu C, Carpenter JF. 2001. A specific molar ratio of stabilizer to protein is required for storage stability of a lyophilized monoclonal antibody. J Pharm Sci 90(3):310–321.
16. Pikal MJ. 1999. Mechanisms of protein stabilization during freeze-drying and storage: The relative importance of thermodynamic stabilization and glassy state relaxation dynamics. Drugs Pharm Sci 96:161–198.
17. Tang XC, Pikal MJ. 2004. Design of freeze-drying processes for pharmaceuticals: Practical advice. Pharm Res 21(2):191–200.
18. Wilhelm C, Gazeau F. 2008. Universal cell labelling with anionic magnetic nanoparticles. Biomaterials 29(22):3161–3174.
19. Kohler N, Sun C, Wang J, Zhang MQ. 2005. Methotrexate- modified superparamagnetic nanoparticles and their intracellular uptake into human cancer cells. Langmuir 21(19):8858–8864.